1-20-2003

Simulating Coronas in Color

Stanley D. Gedzelman

James A. Lock
Cleveland State University, j.lock@csuohio.edu

Simulating coronas in color

Stanley D. Gedzelman and James A. Lock

Coronas are simulated in color by use of the Mie scattering theory of light by small droplets through clouds of finite optical thickness embedded in a Rayleigh scattering atmosphere. The primary factors that affect color, visibility, and number of rings of coronas are droplet size, width of the size distribution, and cloud optical thickness. The color sequence of coronas and iridescence varies when the droplet radius is smaller than ~6-μm. As radius increases to approximately 3.5 μm, new color bands appear at the center of the corona and fade as they move outward. As the radius continues to increase to ~6 μm, successively more inner rings become fixed in the manner described by classical diffraction theory, while outer rings continue their outward migration. Wave clouds or rippled cloud segments produce the brightest and most vivid multiple ringed coronas and iridescence because their integrated drop size distributions along sunbeams are much narrower than in convective or stratiform clouds. The visibility of coronas and the appearance of the background sky vary with cloud optical depth τ. First the corona becomes visible as a white aureole in a blue sky when $\tau \sim 0.001$. Color purity then rapidly increases to an almost flat maximum in the range $0.05 \leq \tau \leq 0.5$ and then decreases, so coronas are almost completely washed out by a bright gray background when $\tau \geq 4$.

OCIS codes: 010.1290, 280.1310, 290.4020, 290.4210, 330.1690.

1. Introduction

Coronas and iridescence are often produced when sunlight or moonlight penetrates optically thin clouds such as altocumulus and cirrocumulus. A corona consists of a bright central aureole surrounded by one or more concentric rings of diminishing light intensity and color purity. The angular size of the rings is more or less inversely proportional to the radius of the cloud droplets and is usually only a few degrees.[1–3] Except in rare cases, a coronas consists of one or two rings at most. Color purity tends to be low, with subdued pastel tones dominating. In gossamer thin cloud segments[4] or fringes consisting of tiny droplets, irregularly shaped iridescence with a play of vibrant colors resembling opals can appear up to 30° or more from the Sun or the Moon.

Bright coronas with vibrant colors and multiple rings are not seen often because stringent conditions must be met for their formation. The scattering angle varies with particle size and shape, so interference that arises from the natural range of droplet or ice particle radii in most clouds tends to wash out the colored rings. Ice particle clouds seldom produce bright coronas because ice crystals have a range of shapes and orientations as well as sizes, and each of these effects tends to wash out coronas.[5,6] Dramatic coronas and vibrant iridescence therefore form only when the cloud has a narrow particle size distribution and most often consists of water droplets rather than ice particles. During periods in spring in some forested or even desert regions, air fills with pollen grains of one dominant species at a time and coronas result because the grains have relatively uniform size and fall with more-or-less the same orientation.[7–9] Gedzelman saw a pollen corona on 31 March at Phantom Ranch at the base of the Grand Canyon, Arizona.

Cloud optical thickness τ affects the visibility of all atmospheric optical phenomena.[10–12] Tenuous clouds ($\tau \leq 0.005$) do not contain enough droplets to produce bright halos or coronas despite the sharp peak in forward scattering. Multiple scattering in optically thick clouds ($\tau \geq 2$) tends to blur any focused optical phenomenon by spreading all colors of light more nearly uniformly around the sky. Optically thick clouds are also likely to have wide particle size distributions. Thus, most bright coronas have $\tau \leq 0.2$ if they are produced by ice particles and $\tau \leq 1.0$ if they are produced by droplets.[5,6]

The classical model of the corona involves diffrac-

S. D. Gedzelman (stan@scisun.sci.ccny.cuny.edu) is with the Department of Earth and Atmospheric Sciences and the Center for Remote Sensing Science and Technology, City College of New York, New York, New York 10031. J. A. Lock (jimandcarol@stratos.net) is with the Department of Physics, Cleveland State University, Cleveland, Ohio 44115.

Received 7 January 2002; revised manuscript received 7 May 2002.

0003-6935/03/030497-08$15.00/0

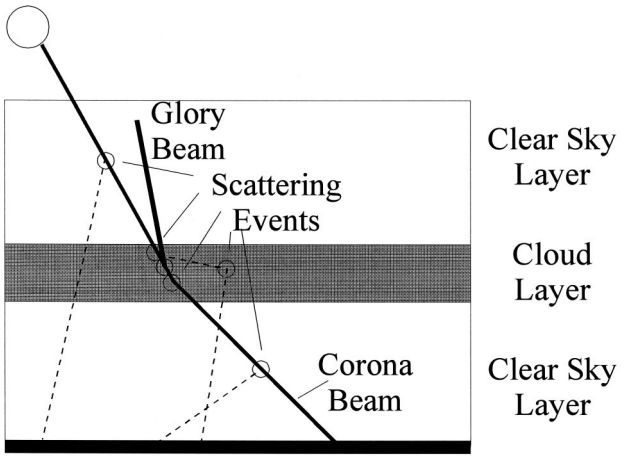

Fig. 1. The three-layer corona cloud model. The corona beam consists of light that reaches the ground after being scattered once in the cloud. The glory beam consists of light that reaches an observer above cloud level after being scattered once in the cloud.

tion of light about small spheres. Lock and Yang[13] developed a more-accurate corona model by applying Mie scattering, which includes transmitted and reflected components of light as well as the diffracted light. They found that, when clouds consist of monodisperse droplets with radius $a \geq 5$ μm, coronas exhibit the color sequences given by the classical diffraction theory. Coronas produced by smaller droplets have color sequences (indicated by chromaticity curves) that vary widely with small changes in droplet size. The theory of Lock and Yang implies that the color sequence of corona rings can be used for estimating droplet size, and that point is enlarged on here.

Existing models of the corona assume perfect, single-scattering clouds in a vacuum and hence either produce more-vibrant coronas than are observed or must overestimate the dispersion of drop sizes to account for the lack of color purity of most coronas. In this paper we extend the Mie theory model of the corona to clouds of finite optical thickness that are embedded in a Rayleigh scattering atmosphere.

2. Corona Model

The corona model consists of a three-layer sandwich, as shown in Fig. 1 and is almost identical to the model used by Gedzelman to simulate glories, as reported in a companion paper.[14] A geometrically thin cloud layer is surrounded by pure, dry air. Cloud height and optical thickness, surface air pressure, and solar zenith angle can all be varied. For the simulations shown here the solar zenith angle is set at 35°. Light beams with 61 wavelengths from 0.4 to 0.7 μm come from the finite-sized Sun (assumed to be a Planck radiator at 5700 K). A random-number generator is used to determine whether and at what level scattering events take place in each layer. Any beam may be scattered more than once in each layer.

When a beam enters the atmosphere it is subject to Rayleigh scattering in the top layer. If the beam reaches the cloud it is subject to Mie scattering by a population of cloud droplets. The wavelength dependence on Mie scattering efficiency and hence on effective optical depth is included. Coronas produced by clouds of nearly spherical ice particles are not considered here but might be simulated by a Mie scattering model with a complex index of refraction because absorption or opacity may account for color differences reported between coronas produced by water droplets and by ice particles.[15]

Once the beam penetrates the cloud, it is again subject to Rayleigh scattering in the lower layer until it reaches the ground. In both layers of clear sky, scattering by aerosols is not included. Aerosols blur atmospheric optical phenomena and reduce their visibility and color purity by brightening and bleaching the background sky, especially near the Sun.

Color dot maps of simulated coronas were made for clouds with droplet radii in the range $1.0 \leq a \leq 10.0$ μm and optical depths in the range $0.002 \leq \tau \leq 10.0$. Significant differences in color and intensity between the top and the bottom of the corona occur only at low solar elevation angles, when scattering reddens sunlight along its oblique path through the atmosphere. Because the Sun is far from the horizon in the simulations presented here, asymmetry is negligible, and all plots represent azimuthal averages of the color dot coronas. We used equal-energy stimulus coefficients to calculate the chromaticity coordinates of the symmetrical coronas and plot chromaticity curves and color maps for the coronas following the approach used by Lock and Yang.[13]

Photographs of coronas (Fig. 2) appear dramatic only if the sky near the Sun is carefully blocked because the gradient of light intensity near the Sun is so large that the outer rings appear almost black compared to the aureole. The human eye is able to overcome this limitation by focusing on small regions of the sky. However, the apparent coloration of coronas is often reduced by intense brightness near the Sun and consequently appears more vivid when brightness is reduced by dark glass or by reflection in water bodies or car windows. Iridescence far from the Sun tends to have more-vivid colors because sky brightness farther from the Sun is more nearly uniform and less intense and because iridescent clouds tend to be optically thin.

A heuristic approach was used to mimic the appearance of simulated coronas on the monitor in photographs in a manner similar to that used by Laven[16] for coronas and glories and by Trankle and Mielke[8] for pollen-generated coronas.[14,17] To correct for the monitor's limited color range and excessive apparent color saturation we reduced the distance r of each point from the tristimulus neutral point ($x = 0.3503$, $y = 0.3616$) to an effective distance $r_{\text{eff}} = r^{1.4}$. To compensate for the monitor's nonlinear response to light intensity we scaled the RGB values for each point by $255 \times (I/I_{\max})^{0.1}$, where $I_{\max}$ is intensity at a radial distance $7.5/a$ shortly inside the corona's first red ring. The exponent used here (0.1) is smaller than the standard gamma correction (0.45) of moni-

(a)

(b)

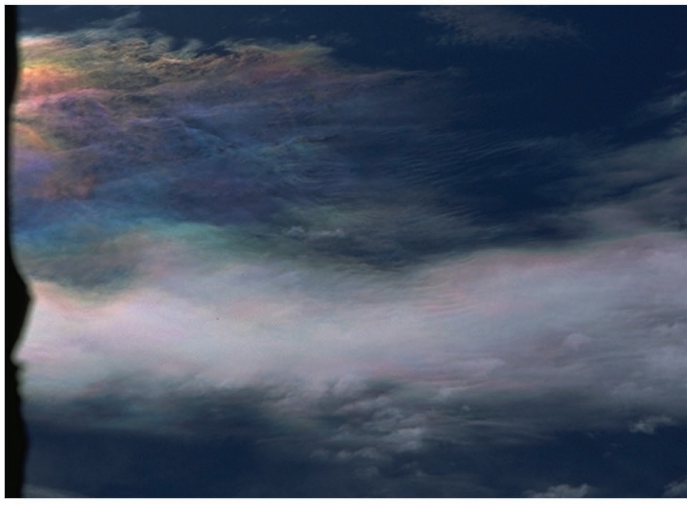

(c)

Fig. 2. Photographs of coronas and iridescence in (a) a thin patch of cirrocumulus in July 1984 over Manhattan, New York; (b) wavy cirrocumulus on 26 December 1993 over Sarasota, Florida, with a hint of a dark blue band; and (c) iridescence in wavy altocumulus on 1 January 2000 over Boynton Beach, Florida.

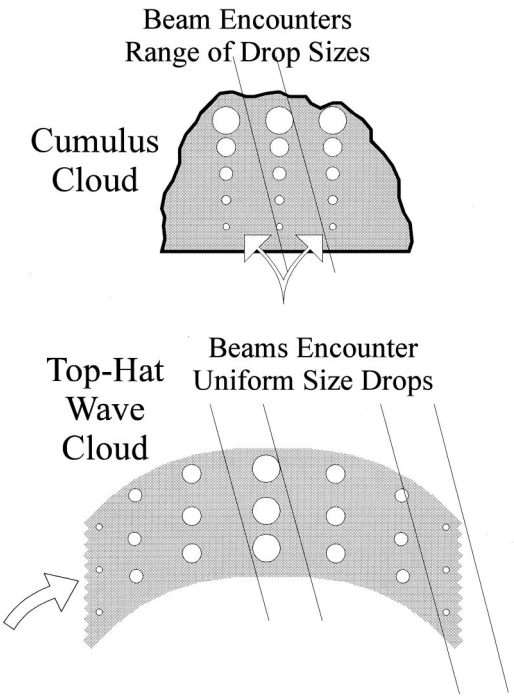

Fig. 3. Schematic diagram showing ranges of droplet sizes encountered by sunbeams passing through a convective cloud and through a wave cloud with a top-hat relative humidity profile.

tors, but it serves to mimic the ability of the human eye to focus on small sections of the sky and consequently produced more visually pleasing results with more rings than most photographs can capture. Finally, to reduce the abruptness of color changes between adjacent rings and best mimic the shimmering, translucent quality of the real phenomena, we gently smoothed the images, using the Micrografx Picture Publisher program.

3. Cloud Types and Droplet Spectra

It has long been recognized that lenticular clouds produce some of the most vivid coronas, and it has been assumed that this is so because those clouds have narrower drop size distributions than most other kinds.[18] For the same reason, altocumulus produce more-vivid coronas and iridescence when they consist of fine ripples than when they are composed of polygonal convection cells, as Fig. 2 suggests.

The relevant drop size distribution for optical phenomena is the integral along a sunbeam through the cloud (Fig. 3). Except at their edges, convective clouds have broad sun-path-integrated droplet size distributions because droplets grow from tiny values near the cloud base to larger values near the cloud top as they rise in the updraft. Wave clouds have horizontally segregated drop size distributions that are almost monodisperse if the vertical structure of relative humidity has a top-hat profile. In that case every height in a vertical slice of the wave cloud has been lifted an equal distance above its condensation level and will have the same-sized droplets until they grow large enough to initiate coalescence.

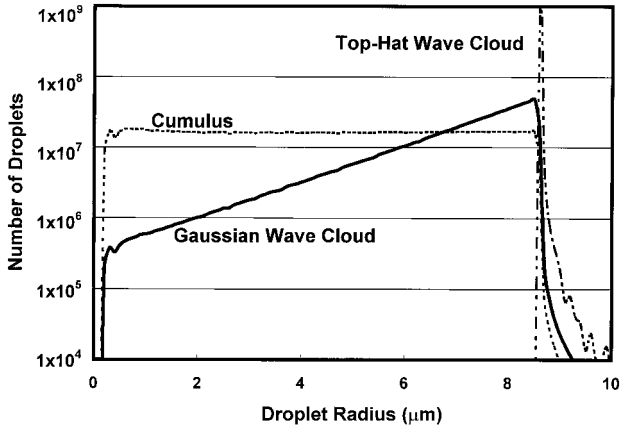

Fig. 4. Droplet size distributions for a convective cloud and for wave clouds with Gaussian and top-hat humidity profiles.

Vertically integrated drop size distributions were generated for optically thin convective and wave clouds by use of a cloud microphysics condensation model similar to that which was developed by Mordy (Fig. 4).[19] The distributions in Fig. 4 were produced by clouds with optical thickness $\tau \approx 0.15$; cloud base, 600 hPa; $T = 10$ °C; and 10^7-m^{-3} cloud condensation nuclei in the range $0.035 \leq a \leq 0.85$ μm, with a number concentration that decreased to a factor of 0.35 for each doubling of particle mass. The convective clouds had flat drop size distributions, which shows why they produce poorly defined coronas. By contrast, wave clouds with Gaussian humidity profiles that approach a top-hat profile have sharply peaked drop size distributions, which is why they produce the most spectacular coronas.

So long as the clouds consist of droplets with radii smaller than ~15 μm, coalescence is not initiated and the drop size distribution remains narrow because it is governed by diffusion. Figure 5 shows the relation between droplet radius and optical thickness τ of a wave cloud that is 10 hPa thick. The results are almost independent of temperature and updraft speed but vary with pressure of cloud base. They

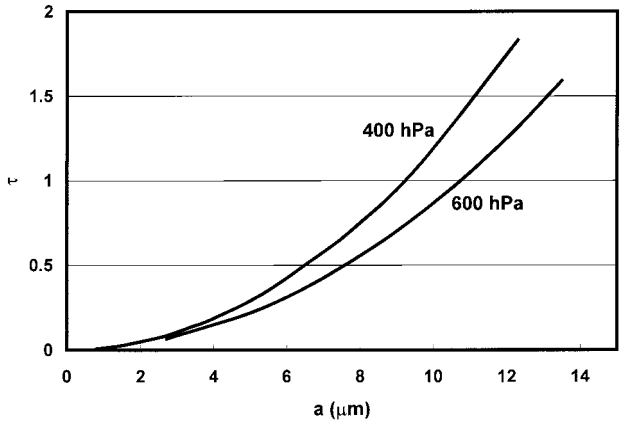

Fig. 5. Relationship between droplet radius and the optical thickness τ of a wave cloud 10 hPa thick. Coalescence begins once optical thickness approaches 2.

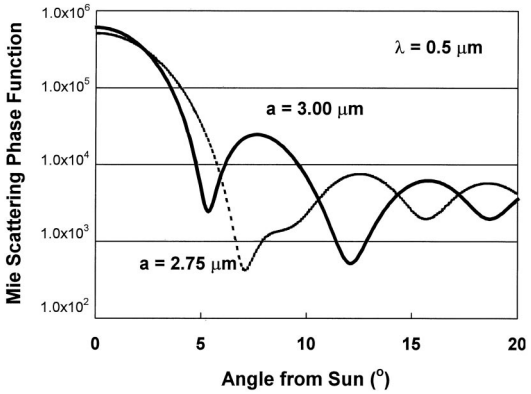

Fig. 6. Mie scattering phase functions for $\lambda = 0.5$ μm and droplets with radii 2.75 and 3.0 μm, showing rapid changes in the shape of the curve.

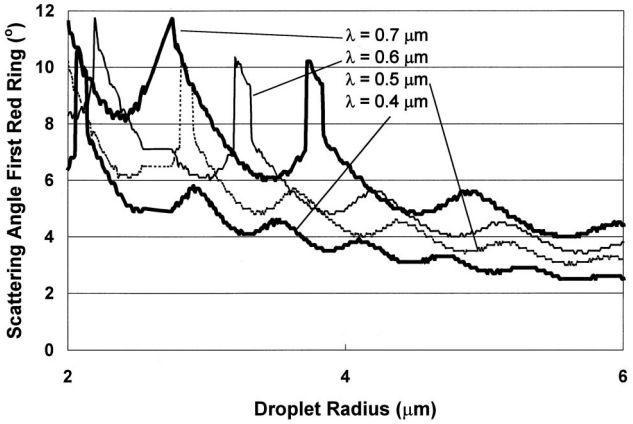

Fig. 7. Deflection angles of the first peak of the Mie scattering phase function for $\lambda = 0.4, 0.5, 0.6, 0.7$ μm as a function of droplet radius. Overlapping of these peaks at small droplet radii illustrates why corona colors vary with droplet radius.

indicate that only clouds with relatively small optical depths produce the small droplets associated with the most vivid coronas and iridescence. Furthermore, once $\tau \geq 2$, not only does multiple scattering seriously reduce corona purity but droplets have grown large enough to initiate coalescence and thereby reduce corona purity further.

4. Results

One of the striking consequences of Mie theory is that the colors of coronas produced by clouds of tiny droplets differ markedly from those given by the classical diffraction theory.[13] A corona produced by droplets with radius $a \geq 6$ μm has pronounced multiple rings and an almost fixed color sequence that is closely approximated by diffraction theory. For smaller droplets the Mie scattering phase function and the total scattering cross section vary rapidly with droplet size. Figure 6 shows that the Mie phase functions for $a = 2.5$ μm and $a = 3.0$ μm are not merely telescoped versions of each other but have a distinct appearance. Figure 7 shows that the scattering angles of the first intensity minima for different visible wavelengths overlap as the result of their large variations when droplet radius is small but begin to settle into a regular pattern once a is larger than ~3.5 μm.

Therefore, coronas and iridescence produced in clouds of droplets with radii smaller than ~3.5 μm experience large differences of color sequences, which are indicated in the color map of Fig. 8 and the chromaticity diagrams of Fig. 9. Figure 8 shows that new color bands form at the inside of the corona and then simultaneously move outward and fade because of increased interference as the droplet radius increases to ~3.5 μm. As the droplet radius increases above ~3.5 μm, successively more inner rings become fixed in the order specified by diffraction theory. Outer color bands continue moving outward and fading as droplet radius increases to ~6.0 μm. This means that the color sequence of visible light coronas can be used to indicate droplet size of the cloud when droplets are small. Extrapolating to the near infrared implies that multichannel sensors can potentially be used to determine droplet size distributions of optically thin clouds remotely from ground level by viewing of coronas in the infrared, as has been done for glories.[20]

Few, if any, complete coronas are produced by droplets with radii smaller than ~3.0 μm because small droplets grow extremely fast by diffusion and appear only when air is lifted a few meters above its

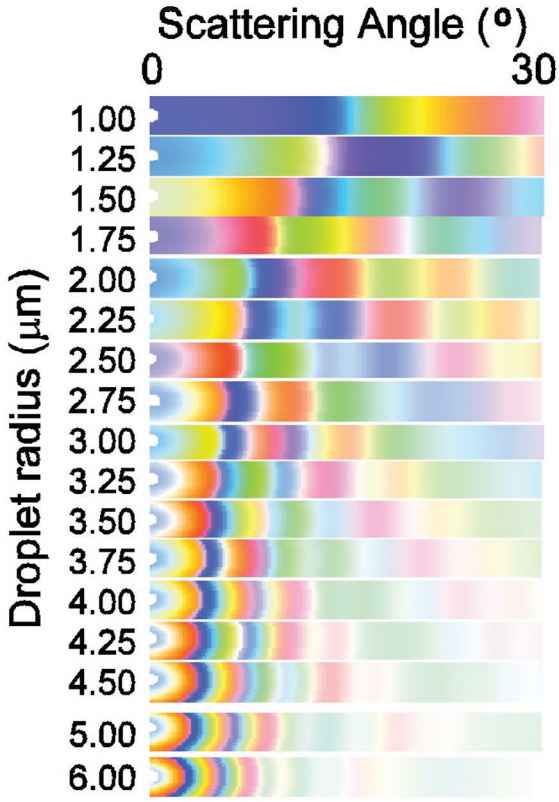

Fig. 8. Color map showing corona colors as a function of droplet radius and scattering angle for a perfect Mie scattering model. The sequence of corona colors changes rapidly for small droplets but becomes fixed once droplet radius exceeds ~6 μm.

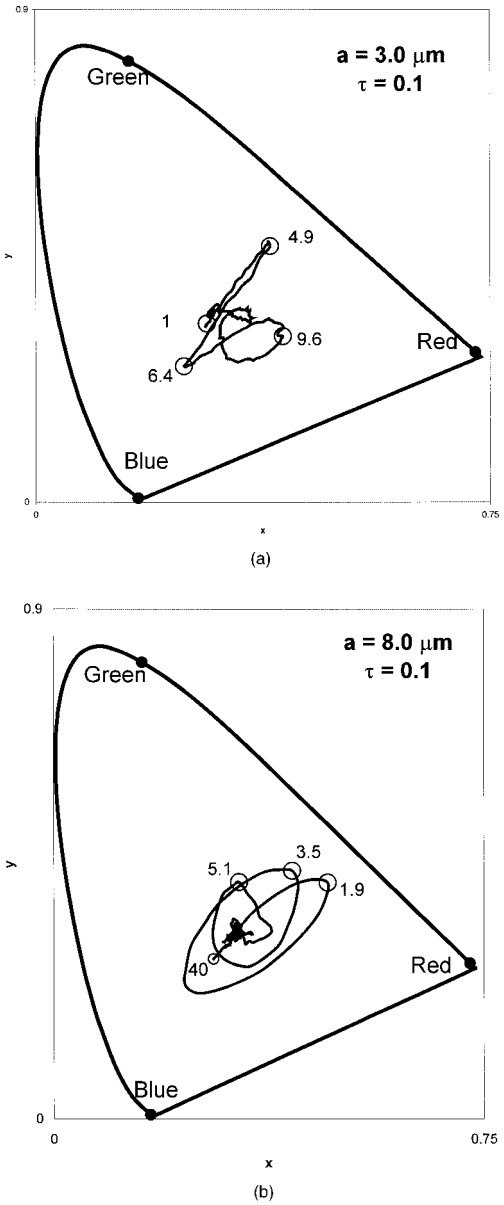

Fig. 9. Chromaticity diagrams for a cloud of optical thickness 0.1 when $a = 3.0$, 8.0 μm. Scattering angles (deg) given for circled points.

condensation level. This makes it extremely unlikely that uniform droplet size can be sustained over a great enough horizontal extent of cloud needed for the large coronas associated with small droplets unless the viewer is close to the cloud. Iridescent patches can, however, sport an extremely lively play of color because these restrictions on droplet size do not apply to the tiny rippled fragments in gossamer thin altocumulus and cirrocumulus.

The color purity of natural coronas rarely approaches the maximum value produced by Mie scattering for a single cloud droplet in vacuum because of multiple scattering and variations of droplet radius. Figure 10 shows how the maximum color purity of the first ring varies with cloud optical thickness when

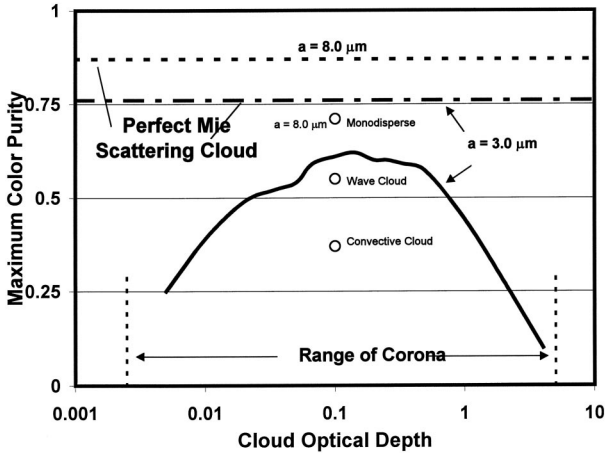

Fig. 10. Maximum color purity of the inner ring of the corona as a function of cloud optical thickness τ for solar zenith angle $Z = 35°$ and droplet radius $a = 3.0$ μm (solid curve, top) compared with maximum color purity given by the perfect Mie scattering model (dashed–dotted curve). Circles indicate maximum color purity for convective cloud, wave cloud, and monodisperse droplet size distributions when the largest droplet has a radius of 8.0 μm at optical thickness 0.1.

droplet radius is 3.0 μm, and Fig. 11 depicts the colors of the corona and the background sky as a function of cloud optical thickness. Tenuous clouds ($\tau \leq 0.005$) contain so few particles that the corona appears as a white aureole in a blue sky. Coronas attain highest color purity and have the largest number of visible rings when optical thickness lies in the approximate range 0.05–0.5. In this range of optical thickness the corona contains a dark blue ring,

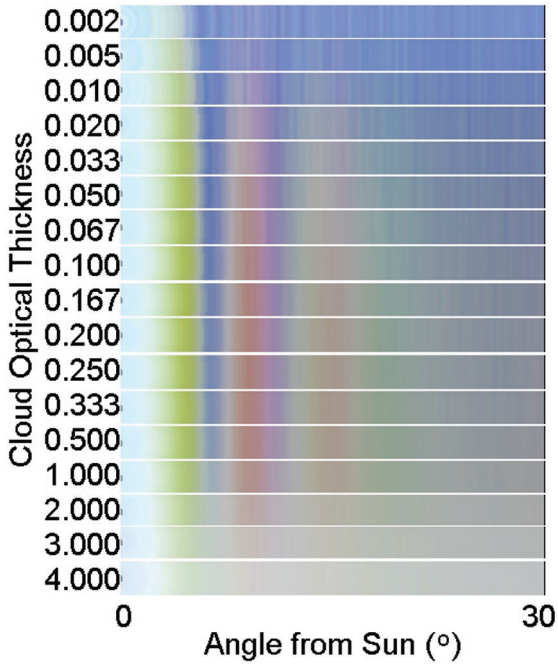

Fig. 11. Color map of coronas as a function of cloud optical thickness and scattering angle for solar zenith angle $Z = 35°$ and droplet radius $a = 3.0$ μm.

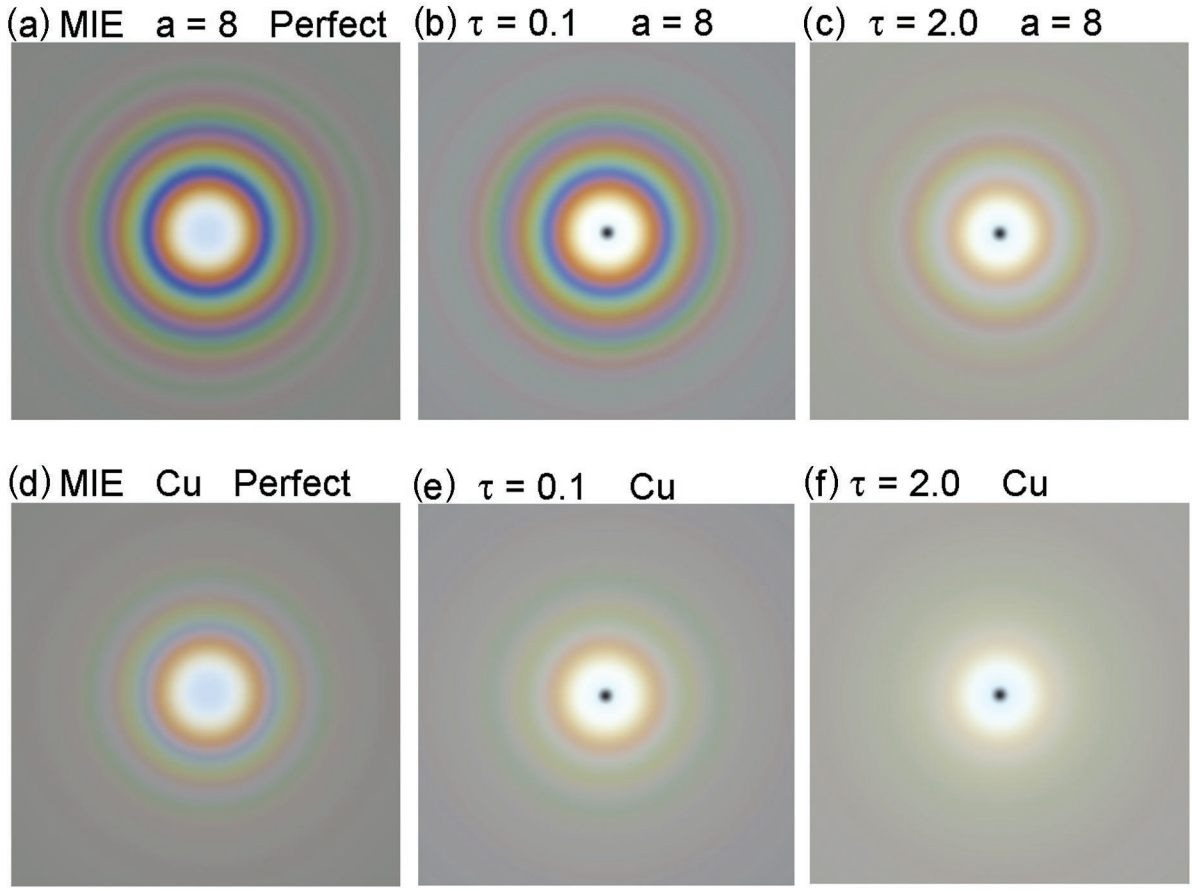

Fig. 12. Color-intensity maps showing the effects of cloud optical thickness and the sharpness of droplet size distribution on the appearance of the corona. The most vibrant, multiringed coronas are produced by optically thin clouds with narrow droplet size distributions. Interference that results from flat and wide droplet size distributions washes out the outer rings, whereas multiple scattering from optically thick clouds blurs the entire corona. A dark blue ring just outside the red ring is present only in optically thin clouds with sharply peaked droplet size distributions.

provided that the droplet size distribution is narrow. Such a dark blue ring can be seen in Nieman's photograph of a corona laced by a contrail taken at Nederland, Colorado.[15] At larger optical thickness, multiple scattering progressively washes out coronas and brightens the gray background sky. Coronas are faint apparitions at best once cloud optical thickness exceeds ~4, and they disappear from view before cloud optical thickness reaches ~10.

Aerosol particles severely reduce the color purity of coronas because they increase the optical depth of the clear air and scatter most light by small angles. This is why sharply defined coronas are almost never seen on hazy days or when a thick layer of humid air is present below cloud base. In the two years following the eruption of Mt. Pinatubo, Gedzelman did not see a single vivid corona.

Coronas are also washed out when clouds have flat, broad droplet size distributions. Figure 12 shows the effect of cloud optical thickness and the sharpness of the droplet size distribution on the appearance of coronas when the largest droplets have a radius of 8 μm. Coronas produced by monodisperse wave clouds with top-hat humidity profiles and optical thickness 0.1 [Fig. 12(b)] are almost as vivid and multiringed as coronas produced by a perfect Mie scattering model and have a dark blue ring just outside the inner red ring. Three or perhaps four red and pale green or yellow rings are still distinctly visible at optical thickness 2 [Fig. 12(c)], but the dark blue ring is gone. Coronas have much lower color purity, fewer visible rings, and no dark blue ring when the droplet size distribution is flat.

Corona color diagrams only realistic appear if the viewer's vision is focused on an extremely small segment of the sky. When a wide-angle view is taken, variations of light intensity make the inner parts of the corona appear bleached while outer portions and regions of clear sky appear almost black by comparison. Indeed, it may well be that iridescent clouds usually have a more pleasing appearance than coronas not only because they consist of smaller droplets with a more varied play of colors but because intensity variations are smaller farther from the Sun.

We are thankful to the participants of the American Meteorological Society's and the Optical Society of America's topical meetings on meteorological op-

tics for sharing their knowledge and love of atmospheric optical phenomena. Several people deserve particular mention here. We have learned much during discussions and correspondence with Ray Lee, Chuck Adler, Michael Vollmer, and Ken Sassen. When this manuscript was in late stages of preparation, we learned of Philip Laven's manuscript,[16] which contains a more-detailed analysis of perfect Mie scattering solutions for the glory and rainbow. Laven and an anonymous reviewer made incisive comments that improved the quality of the paper. This research was supported by NASA Tropical Rain Measuring Mission (TRMM), Professional Staff Congress (PSC), City University of New York and National Oceanic and Aeronautic Administration Center for Remote Sensing Science and Technology (CREST) grants to S. D. Gedzelman and by NASA and National Science Foundation grants to J. A. Lock.

References

1. M. Minnaert, *The Nature of Light and Color in the Open Air* (Dover, New York, 1954), Chap. 10.
2. W. J. Humphreys, *Physics of the Air* (Dover, New York, 1964), Chap. 6.
3. R. A. R. Tricker, *An Introduction to Atmospheric Optics* (American Elsevier, New York, 1970), Chaps 5 and 7.
4. S. D. Gedzelman, "In praise of altocumulus," Weatherwise **41,** 143–149 (1988).
5. K. Sassen, "Corona-producing cirrus cloud properties derived from polarization lidar and photographic analyses," Appl. Opt. **30,** 3421–3428 (1991).
6. K. Sassen, G. G. Mace, J. Hallett, and M. R. Piellot, "Corona-producing ice clouds: a case study of a cold mid-layer cirrus layer," Appl. Opt. **37,** 1477–1485 (1998).
7. P. Parviainen, C. F. Bohren, and V. Makelä, "Vertical elliptical coronas," Appl. Opt. **33,** 4548–4551 (1994).
8. E. Tränkle and B. Mielke, "Simulation and analysis of pollen coronas," Appl. Opt. **33,** 4552–4563 (1994).
9. F. Mims, "Solar corona caused by juniper pollen in Texas," Appl. Opt. **37,** 1486–1488 (1998).
10. S. D. Gedzelman, "Visibility of rainbows and halos," Appl. Opt. **19,** 3068–3074 (1980).
11. S. D. Gedzelman, "Simulating rainbows and halos in color," Appl. Opt. **33,** 4607–4613 (1994).
12. E. Tränkle and R. G. Greenler, "Multiple-scattering effects in halo phenomena," J. Opt. Soc. Am. A **4,** 591–599 (1987).
13. J. Lock and L. Yang, "Mie theory model of the corona," Appl. Opt. **30,** 3408–3414 (1991).
14. S. D. Gedzelman, "Simulating glories and cloudbows in color," Appl. Opt. **42,** 429–435 (2003).
15. J. A. Shaw and P. J. Neiman, "Iridescence and coronas related to cloud particle-size distributions and meteorology," presented at the Seventh Topical Meeting on Meteorological Optics, Boulder, Colo., 5–8 June 2001; preprint available at http://www.asp.ucar.edu/MetOptics/Preprints.pdf.
16. R. J. Kubesh, "Computer display of chromaticity coordinates with the rainbow as an example," Am. J. Phys. **60,** 919–923 (1992).
17. P. Laven, "Simulation of rainbows, coronas, and glories by use of Mie theory," Appl. Opt. **42,** 436–444 (2003).
18. D. K. Lynch and W. Livingston, *Light and Color in Nature* (Cambridge U. Press, New York 1995), p. 124.
19. W. Mordy, "Computations of the growth by condensation of a population of cloud droplets," Tellus **11,** 17–43 (1959).
20. J. D. Spinhirne and T. Nakajima, "Glory of clouds in the infrared," Appl. Opt. **33,** 4652–4662 (1994).